Macromolecules
ARTICLE

Macromolecules **2009**, *42*, 6501–6509 **6501**
DOI: 10.1021/ma900756w

Electrospun Nanofibrous Film Doped with a Conjugated Polymer for DNT Fluorescence Sensor

Yuanyuan Long, Haibo Chen, Yu Yang, Huaming Wang, Yufei Yang, Na Li, Kean Li, Jian Pei,* and Feng Liu*

Beijing National Laboratory for Molecular Sciences, the Key Laboratory of Bioorganic Chemistry and Molecular Engineering of Ministry of Education, College of Chemistry and Molecular Engineering, Peking University, Beijing 100871, China

Received April 7, 2009; Revised Manuscript Received August 3, 2009

ABSTRACT: Electrospun nanofibrous film doped with a fluorescent conjugated polymer **P** was developed as a sensory device for detection of the explosive 2,4-dinitrotoluene (DNT). Polymer **P** obtained through a Sonogashira cross-coupling polymerization showed high affinity and excellent fluorescence quenching property toward electro-deficient compound DNT in solution. A versatile and effective electrospinning technique, which effectively reduced aggregation and fluorescence self-quenching of the conjugated polymers in thin film by the traditional spin-casting, was successfully employed to develop explosive-sensing nanofibrous devices. By doping with polystyrene as supporting matrix and subsequent electrospinning, the obtained fluorescent nanofibrous film exhibited remarkable sensitivity to trace DNT vapor due to a large surface area-to-volume ratio and unique porous structure. The sensitivity of the device was further improved by introducing secondary pores into the nanofibers through addition of a surfactant, sodium dodecyl sulfate, as a porogen agent. This strategy can provide a platform for other conjugated polymers using electrospinning technology to construct new optical chemo- and biosensors.

Introduction

The design and fabrication of chemical sensors have attracted considerable interests for its widely practical and potential applications.[1] Among all kinds of chemosensors, the explosive agents sensors, in which changes in optical properties of sensor matrices engendered upon exposure to vapors have served as output signals, are very important for their versatile applications in homeland safety, industrial process control, environment monitoring, and daily life. To develop efficient chemosensors for the detection of explosive agents, such as DNT and TNT, still is of a challenge.[2] Recently, only a few examples about sensors based on one-dimensional nanofibers for explosive agents were reported.[3] Therefore, to explore novel materials with their unique properties is of great importance in both fundamental research and industry.

Conjugated polymers (CPs) have been proved to be high-performance sensing probes due to their excellent molar absorptivity and fluorescence quantum yields and amplified sensory responses compared with small fluorescent molecules[4] for the analysis of chemical and biomolecules.[5] Poly(iptycenebutadiynylene)[6] and silane−phenylenedivinylene copolymers[7] were developed for explosive vapor detection with high sensory efficiency. Because of the signal amplification effect of CPs, less than parts per million (ppm) level of nitroaromatic explosive vapor can be detected. In principle, polymeric materials can response to several types of electron-deficient compounds although some organic solvent or organic acid may be the interferents.[8] However, selectivity can be improved from their intrinsic nature (polar or nonpolar, aromatic or hydrocarbon, etc.), functional groups, and the presence of well-defined receptors.[6a] Moreover, the self-aggregation behavior of CPs, which leads to serious fluorescence self-quenching, is a major disadvantage counteracting their application in chemical sensors. Electrospinning is a simple and versatile wet fabrication technique for producing ultralong and continuous nano- to microscale fibers.[9] Considerable investigations have focused on the generation of new nanostructured materials, on controlling the surface morphology, and on their applications.[10] The electrospun fibers possess a number of characteristics such as high specific surface area, high aspect ratio, and unique porosity as a result of random deposition of the fibers. It is widely applied to fabricate various functional materials in optoelectronic technology, catalysis, filtration, medicine, and fluorescence chemosensors.[11] Now, it has been reported that fluorescent quantum dots (QDs), which tend to aggregate and their properties are ultrasensitive to environmental variations, can be homogenously distributed into polymer nanofibers with well preservation of optical properties by electrospinning technique.[12] Therefore, the combination of electrospinning with fluorescent CPs offers the potential application as a new and universal fabrication approach for chemosensory devices. The method can be based on ordinary fluorescent CPs which are inclined to self-aggregate in solid through $\pi-\pi$ stacking interaction and generate high sensitivity.

Herein, we report the synthesis and photophysical properties of a novel polymer **P** toward 2,4-dinitrotoluene (DNT). Electrospinning is employed to fabricate nanofibrous film explosive sensing device by doping **P** with a supporting matrix, polystyrene (PS). The morphology and fluorescence property of the nanofibrous film are investigated, and the sensing performance toward DNT is explored. Moreover, sodium dodecyl sulfate (SDS) is added as a porogen to enlarge the surface area and generate secondary porous structure to the nanofibrous film, so as to further improve the sensitivity. Such fluorescence sensor, to the best of our knowledge, is the first example to employ electrospun conjugated polymer fibrous membrane for explosive detection. This method has potential applications in both the fabrication of

*Corresponding author. E-mail: liufeng@pku.edu.cn (F.L.); jianpei@pku.edu.cn (J.P.).

Published on Web 08/14/2009

Scheme 1. Synthesis of Conjugated Polymer P

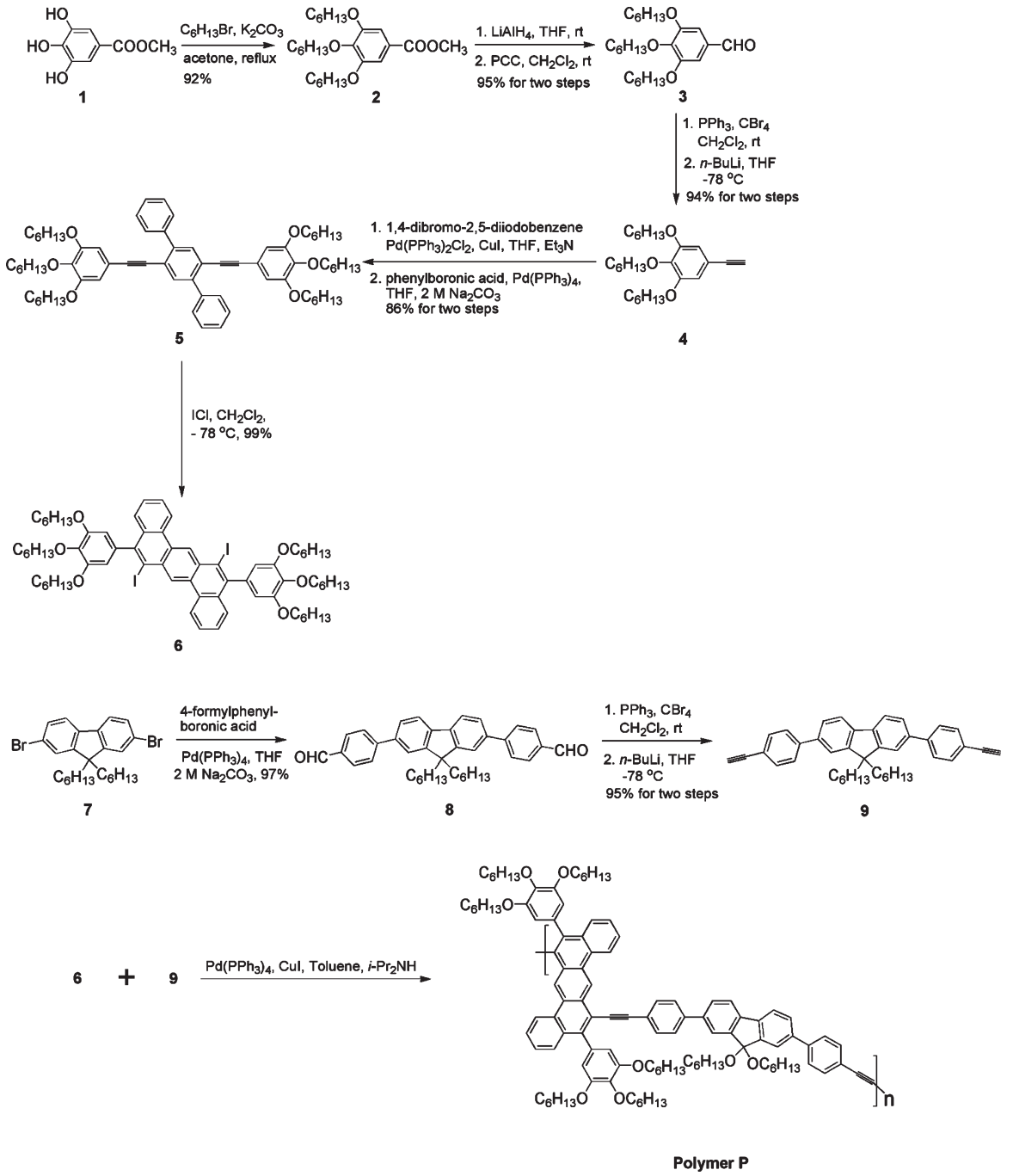

sensing devices based on wide range of CPs and the detection of other electron-deficient species.

Results and Discussion

Synthesis and Characterization of Polymer P. Scheme 1 illustrates the synthetic approach to polymer **P**. Alkylation of methyl gallate (**1**) with 1-bromohexane in present of K_2CO_3 afforded compound **2** in 88% yield. A reduction reaction of **2** using $LiAlH_4$ followed by an oxidation gave aldehyde **3** in high yield (95% for two steps). Reduction of **2** using $LiAlH_4$ followed by the same oxidation gave aldehyde **3** in 95% yield (overall two steps). A Corey−Fuchs reaction of aldehyde **3** afforded alkyne **4**. A Sonogashira reaction between alkyne **4** and 1,4-dibromo-2,5-diiodobenzene with catalyst $Pd(PPh_3)_2Cl_2$ followed by a Suzuki coupling reaction with phenylbronic acid using $Pd(PPh_3)_4$ as catalyst gave compound **5** in 86% yield. Polycyclic aromatic hydrocarbon iodide monomer was prepared in almost quantitative yield following the classical procedure via ICl-induced intramolecular cyclization of **5**.[13]

Diyne **9** was prepared through a Suzuki reaction of 2,7-dibromo-9,9-dihexylfluorene (**7**) with 4-formylphenylboronic acid followed by the Corey−Fuchs reaction in 92% yield (overall three steps). A palladium-catalyzed Sonogashira cross-coupling polymerization between the diiododibenz-[*a*,*h*]anthracene (**6**) and diyne **9** afforded polymer **P** as a yellow fiber in 56% yield. The crude polymers were washed with methanol, water, and methanol again, successively, placed in a Soxhlet apparatus and extracted with refluxed acetone for 48 h, and then dried at 60 °C in a vacuum oven.

Polymer **P** was readily soluble in common organic solvents such as chloroform, THF, and toluene. Its molecular structure and the purity were verified by ^{1}H and ^{13}C NMR, elemental analysis, and Fourier transform infrared (FT-IR) spectroscopy. The GPC analysis indicated that the number-average molecular weight (M_n) of polymer **P** was 18 000 (DP 10) with 1.9 polydispersity index (PDI).

Fluorescence Response Characteristics of P to DNT in Solution. CPs showed very high sensitivity to electron-deficient analytes such as nitroaromatic explosives via a photoinduced electron-transfer quenching mechanism.[2a−2c] It is instructive to investigate the fluorescence response behavior of **P** in solution, from which the relative affinity of individual polymer chain to the analyte can be evaluated.[5a] Figure 1 illustrates the absorption, excitation, and emission spectra of polymer **P** in dilute $CHCl_3$ solution (5×10^{-6} M). The absorption maximum λ_{max} in dilute solution showed several peaks between 250 and 450 nm. Upon excitation at 327 nm, which is the characteristic absorption peak of dibenz[*a,h*]anthracene, the emission maximum λ_{max} of **P** peaked at 427 and 453 nm in dilute solution. Using 9,10-diphenylanthracene in cyclohexane as standard ($\Phi_F = 1.00$), the quantum yield of **P** in chloroform was determined to be 0.30.

The fluorescence response of **P** to 2,4-dinitrotoluene (DNT) as a representative nitroaromatic explosive was systematically studied in chloroform solution. As shown in Figure 2a, it is observed that the emission intensity of **P** in solution was remarkably decreased with the introduction of DNT and decreased gradually with the increase of DNT concentration, which suggested that **P** exhibited a certain extent of sensitivity toward DNT. The relative fluorescence intensity of **P** was plotted as a function of DNT concentration (Stern−Volmer plot, as shown in Figure 2b). It was noticeable that **P** gave rise to nonlinear curves (positive curvatures) in its Stern−Volmer curve. Generally, there are two possible conditions under which fluorophore exhibits nonlinear Stern−Volmer plot: (1) the combined effect of both static and dynamic quenching process; (2) the formation of a complicated system between the host and the quencher, instead of a simple one-to-one dark complex. For these quenching systems, the following two equations are usually used to quantify the experimental data and calculate the quenching constants.

$$F_0/F = (1 + K_D[Q])(1 + K_S[Q]) \quad (1)$$

$$F_0/F = (1 + K_D[Q]) \exp(V[Q]) \quad (2)$$

in which F_0 and F represent the fluorescence intensities in the absence and presence of the quencher, respectively. K_D is the dynamic quenching constant, K_S and V denote the static quenching constant, and [Q] is the quencher concentration. $1 + K_D[Q]$ represents the contribution from the dynamic quenching, and $1 + K_S[Q]$ or $\exp(V[Q])$ implies the part of the static quenching. Equation 1, in which the term of static quenching is a linear function of quencher concentration [Q], can be applied to systems when the fluorophore and the quencher form a simple one-to-one dark complex. In such cases, K_D corresponds to the association constant of the fluorophore and quencher. Equation 2 can be used for systems with more complex species, in which the static quenching profile deviates from the linear function.

The fluorescence lifetime is closely associated with the collision deactivation of the fluorophore. As a result, with the addition of quencher, the fluorescence lifetime should diminish in dynamic quenching, while invariant in static quenching. Therefore, monitoring the lifetime change can provide a direct means to infer the type of fluorescence quenching and determine the dynamic quenching constant

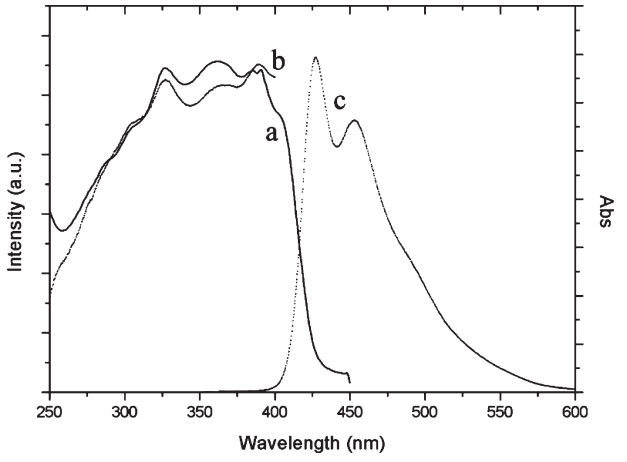

Figure 1. Absorption spectrum of **P** (a), and excitation (b), and emission (c) spectra of **P** in $CHCl_3$ solution (5×10^{-6} M).

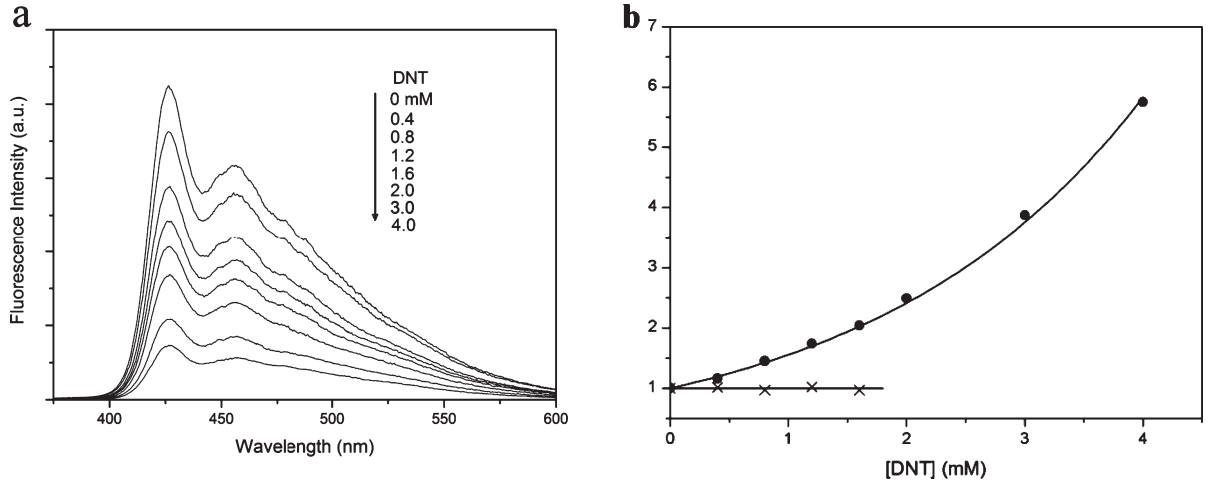

Figure 2. (a) Fluorescence spectra change of **P** as a function of DNT concentration in chloroform: [**P**] = 2×10^{-7} M; [DNT] = 0−4.0 mM (from top to bottom). (b) Stern−Volmer plot of **P** in response to DNT: (●) F_0/F, (×) τ_0/τ.

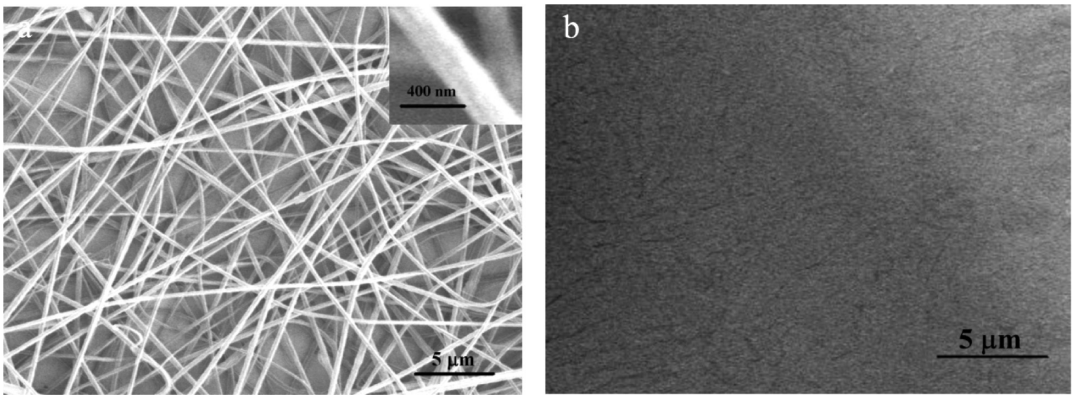

Figure 3. SEM images of the (a) electrospun nanofibrous film and (b) spin-casting film. The electric voltage is 25 kV, and the collecting distance is 25 cm.

independent of the static quenching. Equation 3 expresses the correlation of lifetime with quencher concentration.

$$\tau_0/\tau = 1 + K_D[Q] \quad (3)$$

The fluorescence lifetime for **P** was therefore in the presence of different concentrations of quencher, and the data were fitted to eq 3. As shown in Figure 2b, P showed undetectable fluorescence lifetime change by adding DNT. This phenomenon suggested that static quenching was the dominant mechanism for the present **P**−DNT system, and the ground-state complex was formed between polymer **P** and DNT. Since the dynamic quenching was negligible in the **P**−DNT system, the obtained nonlinear Stern−Volmer plot was in accordance with the latter case mentioned above, which involves the formation of a complicated system between **P** and DNT. Specifically speaking, **P** interacted with more than one DNT molecules to form a dark complex. Applying eq 3 and $K_D = 0$ to eq 2, the static constant V can be evaluated by eq 4.

$$F_0/F = \exp(V[Q]) \quad (4)$$

By fitting experimental data to eq 4, the static quenching constant V was determined to be $440 \pm 2\ M^{-1}$. This value was larger than that in poly(*p*-phenyleneethynylene)−DNT system ($V = 26\ M^{-1}$),[5a] which suggested that a rather strong ground-state complexation was formed between **P** and DNT. The enhanced association may be attributed to the strong tendency of the electron-rich polycyclic backbone of **P** to interact with electron-deficient DNT via electrostatic and $\pi-\pi$ stacking interactions. The results above indicate that polycyclic polymer **P** synthesized in this work exhibits appropriate affinity for the explosive DNT and has potential as sensing agent to be applied to fluorescence sensor.

Fabrication of P-Doped Nanofibrous Sensing Films. On account of molecular weight and solubility limitations of **P**, it could not be electrospun directly. The most effective strategy to improve its spinnability was to dope **P** with other spinnable polymer acting as supporting substrate.[9] Therefore, the choice of substrate polymer should meet the following requirements: (1) The supporting polymer needs to have strong hydrophobicity so that **P** can be well dispersed without aggregation. (2) The supporting polymer should have negligible fluorescence emission in the measured wavelength region, not to interfere with the fluorescence measurement. (3) There must be a proper common solvent that is capable of dissolving both components and is suitable for electrospinning.

We finally selected polystyrene (PS) as the supporting substrate upon consider of the structures, the fluorescence characteristics, and the solubility of **P** and the blending polymer. There were phenyl groups in the PS side chains, which might interact with the rigid backbone of **P** through $\pi-\pi$ stacking to reduce the formation of the **P** aggregates. Meanwhile, the blank electrospun PS nanofibrous film had negligible fluorescence emission in the wavelength region investigated. Moreover, a common solvent dimethylfomamide (DMF) could well dissolve both **P** and PS, acting as an applicable electrospinning solvent. The influences of supporting polymer concentration, voltage, and needle−collector distance were extensively investigated. The electrospinning condition was fixed at 25 kV of voltage and 25 cm of distance with the PS concentration 0.12 g mL^{-1}, under which the obtained fibers showed smooth morphology and small uniform diameter. The scanning electron microscope (SEM) image of the electrospun **P**-doped nanofibrous film is shown in Figure 3a. It was observed that the diameters of fibers were from 300 to 400 nanometers and showed uniform and smooth morphology without beads formation. Because of the disorderly arrangement of the nanofibers, porous structure was formed in the electrospun nonwoven film, which provided a surface area-to-volume ratio roughly 1−2 orders of magnitude higher than that of continuous spin-casting film (shown in Figure 3b).[14] The high surface area-to-volume ratio and unique porous structure were beneficial for sensing application.

To improve the sensitivity, porogen was introduced into the electrospun system to further increase the surface area-to-volume ratio. In **P**-doped electrospun system, surfactant SDS was chosen as a porogen agent added into the electrospun solution. This surfactant-containing solution showed excellent spinnability in the electrospinning process, indicating that the addition of surfactant porogen would not interfere with the electrospinning property. After being aged at 60 °C for 4 h, the porogen molecules could be removed easily by a simple solvent extraction process using deionized water, obtaining hierarchical nanostructured fibers containing pores generated by SDS.

Characterization of Polymer P-Doped Films. The fluorescence spectra of spin-casting film made from a solution of **P** in $CHCl_3$ and electrospun blank PS and **P**−PS nanofibrous films are shown in Figure 4. Because of the high viscosity, no transparent film could be obtained by spin-casting the **P**−PS solution. The fluorescence emission of **P** in $CHCl_3$ solution (10^{-6} M) was recorded for comparison, too. Fluorescence emission was not observed in the blank PS nanofibrous film, so the existence of PS would not interfere with the fluorescence measurement of **P**. Note the fluorescence emission of

P in spin-casting film displaying a dramatic red shift relative to solution, which was due to the aggregation through $\pi-\pi$ stacking interactions. However, the emission features of electrospun **P**−PS film showed minor difference from that in dilute solution, indicating effective prevention of direct contact and aggregation of the conjugated backbones. This indicated that both the supporting polymer PS and the electrospinning treatment significantly avoided the interchain interactions of **P**. Because of the greatly enlarged surface areas of the electrospun fibers and the applied electric field,[9] the solvent evaporation rate of the polymer solution in the electrospinning process was much faster than that in spin-casting. As a result, the polymer chains are quickly frozen, and the conjugated polymers are confined to a dispersed location before they reach $\pi-\pi$ stacking state.

To visualize the fluorescence properties of the electrospun nanofibrous film and spin-casting film, fluorescence microscopy was adopted. The fluorescence images of the two different films are shown in Figure 5. For the electrospun film, the deep blue fluorescent nanofibers were observed distinctly, indicating the well incorporation of **P** into the electrospun nanocomposite. While for the spin-casting film prepared with the **P**−$CHCl_3$ solution, a continuous, dense, and blue-green film was seen.

Response Properties of the P-Doped Sensing Films To Trace DNT Vapor. To verify the validity of the sensing films, the response properties of the fluorescent films toward explosive vapor were extensively examined. The fluorescence quenching experiments with DNT vapor were conducted as follows.[5a] Quartz cell with cover was filled with a small amount of solid DNT and set overnight to ensure saturation vapor pressure of DNT had been reached. The cell was placed in the fluorescence spectrometer, and the glass slide coated with sensing film was immediately inserted into the cell. The emission data were collected every certain time in the wavelength region of 350−600 nm with an excitation wavelength of 327 nm. The time dependence of photoluminescence quenching was observed for all types of sensing films upon exposure to trace DNT vapor, as shown in Figure 6. As expected, the electrospun film showed higher sensitivity toward DNT vapor than the spin-casting film. For example, the nanofibrous film lost nearly 20% of fluorescent intensity after 10 min of exposure, and this value increased to 50% with the exposure continues to 1 h. On the contrary, the dense film of spin-casting showed minor fluorescence quenching (about 5%) in the same period of exposure.

We further improved the sensitivity by introducing pores into the nanofibers so that the surface area of the fibrous film can be increased tremendously and the transport properties of analytes can be considerably improved.[11] Figure 6 shows that the improvement of quenching sensitivity is notable. The fluorescence intensity of the porous nanofibers dropped ~40% after exposure for 10 min, which was almost 2-fold as sensitive as the fibers without pores. After 1 h exposure, nearly 75% of fluorescence of nanofibers had disappeared.

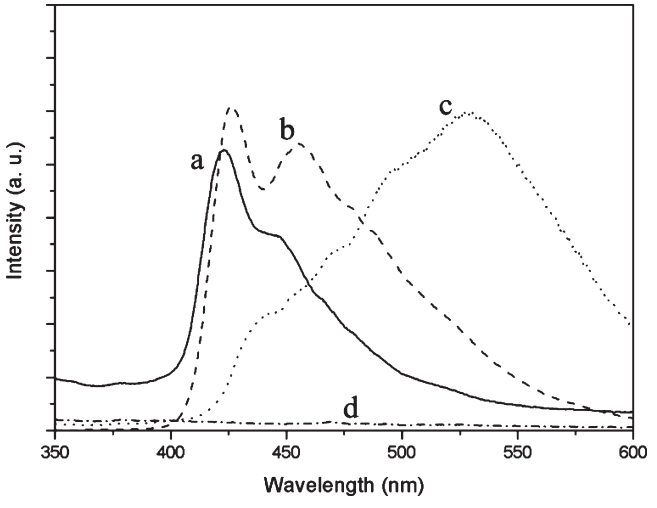

Figure 4. Comparison of fluorescence spectra of **P**−PS nanofibrous film (a), **P** in $CHCl_3$ solution (b), spin-casting film (c), and PS nanofibers (d).

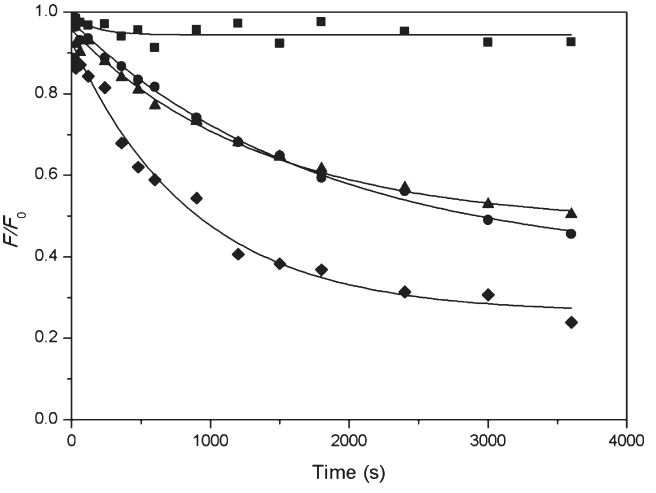

Figure 6. Time-dependent fluorescence quenching of the sensing films upon exposure to DNT vapor: (●) **P**-doped PS nanofibrous film, **P**-doped PS nanofibrous films with porogen (▲) before and after (◆) solvent extraction, and (■) dense film obtained by spin-casting.

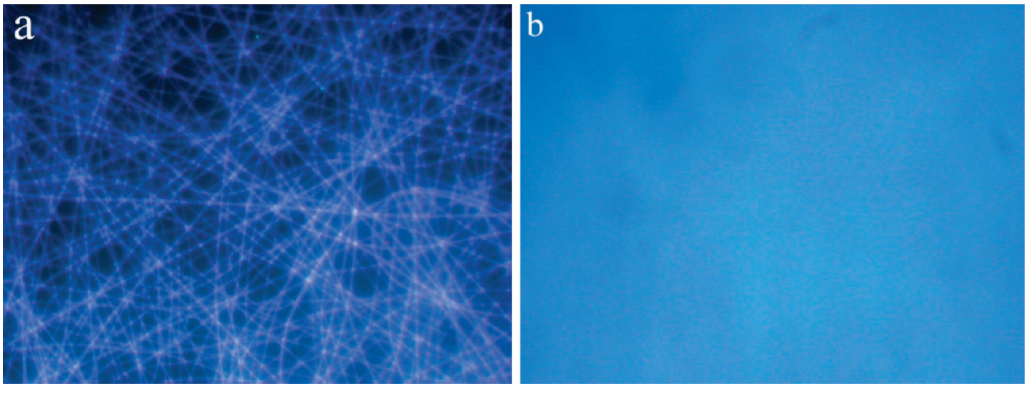

Figure 5. Fluorescence images of the (a) electrospun nanofibrous film and (b) spin-casting film.

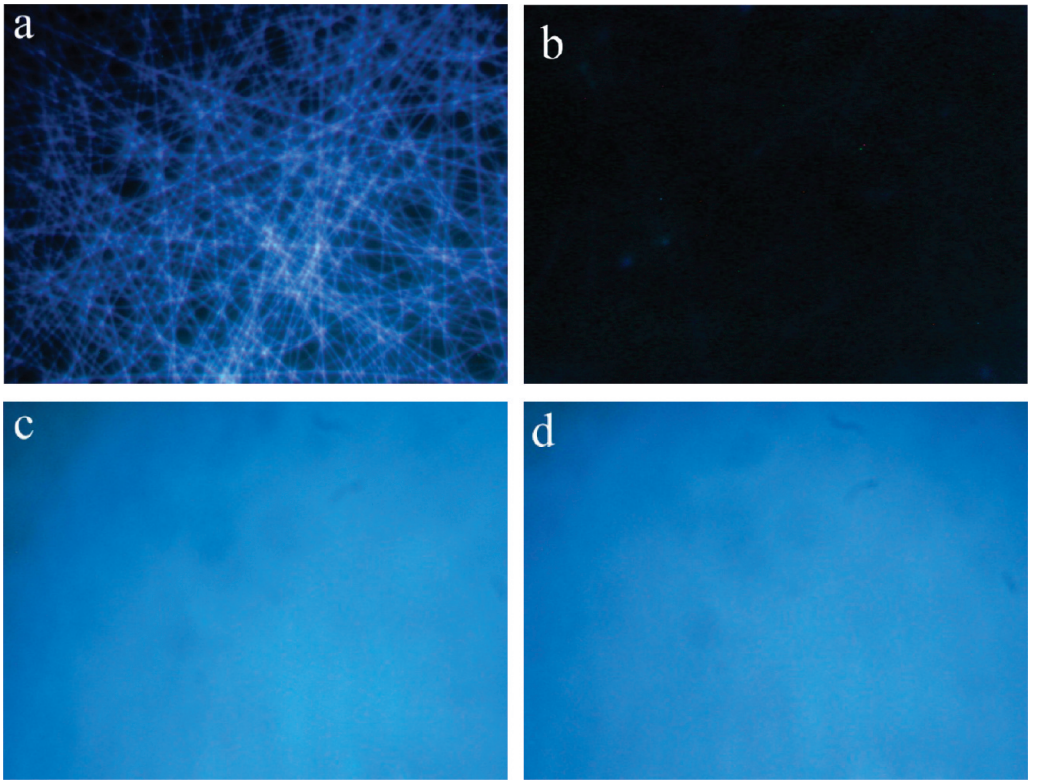

Figure 7. Fluorescence images of electrospun nanofibers with porogen (a) before and (b) after being exposed to DNT vapor for 30 min and dense spin-casting film (c) before and (d) after being exposed to DNT vapor for 30 min.

This efficient quenching is clearly visible using fluorescence microscopy (Figure 7). In a control experiment, the fluorescence images of spin-casting film before and after the DNT exposure were taken and shown in Figure 7. There was hardly any difference observed from this densely packed sensing film.

The remarkable sensing performance observed here was mainly due to the following reasons. First, polymer **P** acting as a fluorescence probe presented relatively large affinity for the nitroaromatic compound DNT, which could be proved from the rather large static quenching constant. This affinity was mainly based on photoinduced charge transfer and $\pi-\pi$ stacking interaction and could provide a strong driving force for fast fluorescence quenching. Second, the electrospun nanofibrous sensing film possessed comparatively large surface area, in which more recognition elements were located on the surface. Moreover, the BET surface areas of nanofibers produced with and without surfactant were measured to be 11.39 and 41.64 $m^2\ g^{-1}$, respectively. According to the increase of surface area and sensitivity, we implied that the addition of surfactant porogen further increased the surface area-to-volume ratio and provided secondary porous structure into the nanofibers. This unique double-stage porous structure could greatly accelerate the targets to diffuse close to the sensing elements and increase the quenching efficiency.

The sensor reported here is reversible. After immersing in ammonia for 20 min followed by drying in air, the fluorescence intensity can be almost entirely recovered and the film can be further used. As illustrated in Figure 8, after five times of quenching and regeneration, the nanofibrous film showed less than about 25% loss of signal intensity than the initial state, indicating good reversibility of the sensor. In addition, when placed in air, the sensor showed good fluorescence stability, and almost no photobleaching was observed during the whole experiment.

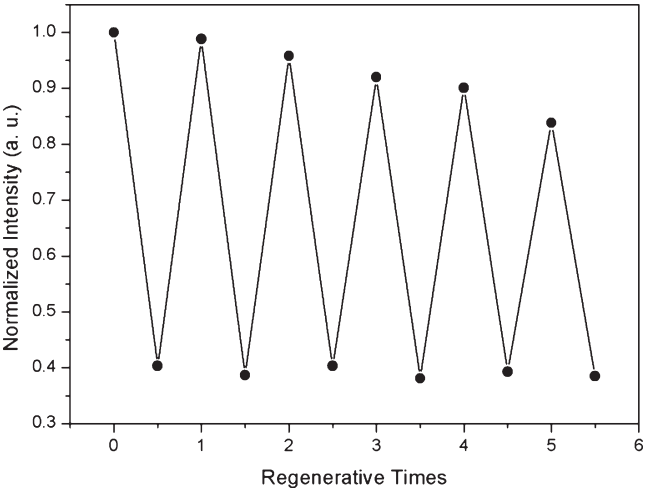

Figure 8. Effect of regenerative times on the DNT quenching efficiency of the nanofibrous film. Quenching time: 30 min, regenerated by immersing into ammonia (0.05 M) for 20 min.

Conclusion

In summary, high-quality polymer nanofibers with uniform morphology have been prepared by electrospinning technology from polymer **P** as excellent fluorescence chemosensor for the detection of electron-deficient nitroaromatic explosive. The nanofibrous sensing film adequately maintained the fluorescence property of polymer **P** and showed higher sensitivity toward the explosive vapor compared to the conventional spin-casting film, indicating that this approach effectively avoided the aggregation of the conjugated polymer. By introducing surfactant SDS as porogen into the fibers, the sensing performance of the nanofibrous film could be further improved.

This strategy showed a promising alternative for developing high-performance explosive sensing devices, which not only gave a successful example of the combination of polycyclic polymer and electrospinning technique for the detection of explosive war agents but also provided a new platform for fluorescence chemosensors adopting common conjugated polymers as probes. It is expected that the electrospinning method will be applicable to the preparation of nanofibers for chemosensors from more conjugated polymers and will make possible the large-scale synthesis of the functional nanofibers with practical applications.

Experimental Section

All chemicals were analytical reagent grade and used as received without further purification. ^{1}H and ^{13}C NMR spectra were recorded on a Varian Mercury 200 MHz or Mercury plus 300 MHz (Varian, Palo Alto, CA) using $CDCl_3$ as solvent unless otherwise noted. All chemical shifts were reported in parts per million (ppm), ^{1}H NMR chemical shifts were referenced to TMS (0 ppm) or $CHCl_3$ (7.26 ppm), and ^{13}C NMR chemical shifts were referenced to $CDCl_3$ (77.00 ppm). The molecular weight of **P** was measured by using a gel permeation chromatography (GPC) system (Waters, MA). Absorption spectra were performed on a U-3010 UV−vis spectrophotometer (Hitachi, Tokyo, Japan). Photoluminescent (PL) spectra were carried out on an F-4500 fluorescence spectrometer (Hitachi, Tokyo, Japan). Elemental analysis was performed using a Vario EL III elemental analyzer (Elementar, Germany). The morphology of the fibers was observed with an S-4800 scanning electron microscope (SEM) (Hitachi, Tokyo, Japan). The fluorescence images were taken on a DMLS fluorescence microscope (Leica, Germany). The surface areas of the nanofibers were measured with an ASAP-2010 apparatus (Micromeritics) and with BET plot. The FT-IR characterization was carried with a VECTOR22 FT-IR spectrometer (Bruker, Germany).

Preparation of P-Doped PS Nanofibrous Films. **P** storage solution was prepared by conjugated polymer **P** (5 mg) dissolved into DMF (2 mL). PS (120 mg), **P** solution (0.5 mL), and DMF (0.5 mL) were mixed and stirred to obtain homogeneous solution in a flask for further electrospinning. For the preparation of nanofibers with porous structure, the same ingredients were adopted with the addition of SDS (5 mg) as porogen. The prepared solution was transferred into a 20 mL syringe mounted on the homemade electrospinning setup. Typically, electrospinning was performed at a voltage of 25 kV, with a distance of 25 cm between the needle and the collector. The flow rate of the solution was controlled by a syringe pump at a constant rate of 0.6 mL h^{-1}. Continuous polymer nanofibers were collected on glass slides mounted on aluminum foil to form fibrous film. The electrospun films were dried in an oven at 60 °C for 12 h to remove organic solvents. In the case of the porous nanofiber film, the porogen (SDS) was extracted by immersing the fibrous film in deionized water for 4 h. For comparison, spin-casting film was also prepared on glass cover slide from chloroform solution of **P** (1 mg mL^{-1}).

2: 1-Bromohexane (26.9 mL, 163 mmol) was added to a mixture of anhydrous K_2CO_3 (22.5 g, 163 mmol) and methyl gallate (5.0 g, 27.2 mmol) in acetone. The resulting suspension was stirred for 24 h at 80 °C. The solid was isolated from the mixture by filtration. The solution was collected and dried over anhydrous Na_2SO_4. After removal of the solvent under reduced pressure, the crude residue was purified using column chromatography (silica gel, ethyl acetate/petroleum ether = 1:30 as eluent) to afford **2** (10.4 g) as a colorless liquid. Yield: 88%. ^{1}H NMR ($CDCl_3$, 300 MHz, ppm): δ 7.25 (1H, s, Ar−H), 4.04−3.99 (6H, m, CH_2O), 3.89 (1H, s, $COOCH_3$), 1.84−1.77 (6H, m, CH_2), 1.51−1.27 (18H, m, CH_2), 0.93−0.88 (9H, m, CH_3). ^{13}C NMR ($CDCl_3$, 75 MHz, ppm): δ 153.1, 153.0, 137.1, 136.2, 106.8, 105.0, 73.3, 69.0, 68.9, 65.2, 31.7, 31.5, 30.1, 29.3, 25.7, 22.6, 22.5, 14.0, 13.9. MS (EI), m/z: 436 (M^+, 100%). HRMS (EI): calcd for $C_{26}H_{44}O_5$: 436.3189. Found: 436.3190.

3: A mixture of $LiAlH_4$ (1.69 g, 34.4 mmol) and THF (80 mL) was stirred at 0 °C, and then a solution of **2** (10.0 g, 22.9 mmol) in 40 mL of anhydrous THF was added dropwise. The mixture was stirred at room temperature for 3 h. Then saturated Na_2SO_4(aq) was added dropwise at 0 °C. The mixture was filtrated, and the solution was collected. Removal of solvent at reduced pressure give a white paste (9.00 g). To a mixture of PCC (7.50 g, 34.2 mmol) and CH_2Cl_2 (80 mL) was added the product above (9.00 g, 22.1 mmol) in 30 mL of CH_2Cl_2 at 0 °C. The mixture was stirred at room temperature overnight. After the solvent was removed at reduced pressure, the residue was purified by a chromatography on silica gel using ethyl acetate/petroleum ether = 1:20 to give **3** as a colorless liquid (8.83 g). Yield: 95% for two steps. ^{1}H NMR ($CDCl_3$, 300 MHz, ppm): δ 9.83 (1H, s, Ar−CHO), 7.08 (2H, s, Ar−H), 4.08−4.02 (6H, m, CH_2O), 1.88−1.73 (6H, m, CH_2),1.53−1.30 (16H, m, CH_2), 0.93−0.89 (9H, m, CH_3). ^{13}C NMR ($CDCl_3$, 75 MHz, ppm): δ 191.2, 153.5, 143.7, 131.4, 107.7, 73.5, 69.1, 31.6, 31.5, 30.2, 29.1, 25.7, 25.6, 22.6, 22.5, 14.0, 13.9. MS (EI), m/z: 406 (M^+, 100%). HRMS (EI): calcd for $C_{25}H_{42}O_4$: 406.3083. Found: 406.3085.

4: A mixture of CBr_4 (13.1 g, 39.4 mmol) and PPh_3 (21.2 g, 80.8 mmol) in 60 mL of CH_2Cl_2 was stirred at 0 °C for 1 h, and then a solution of **3** (8.00 g, 19.7 mmol) in 30 mL of CH_2Cl_2 was added dropwise. The mixture was stirred at room temperature overnight. After filtration, the solution was collected. After the removal of solvent at reduced pressure, the residue was purified by a chromatography on silica gel using ethyl acetate/petroleum ether (1:40) to give a colorless liquid (10.8 g). To a solution of the product above (10.8 g, 19.2 mmol) in 80 mL of anhydrous THF was added *n*-BuLi (23.0 mL, 57.6 mmol) at −78 °C. After at −78 °C for 3 h, the mixture was quenched with NH_4Cl(aq). The aqueous layer was extracted with ethyl acetate. The combined organic extracts were washed with brine and dried over Na_2SO_4. After removal of the solvents under reduced pressure, the residue was purified by a chromatography on silica gel using CH_2Cl_2/petroleum ether (1:4) to give **4** as a colorless liquid (7.83 g, 19.1 mmol). Yield: 96% for two steps. ^{1}H NMR ($CDCl_3$, 300 MHz, ppm): δ 6.69 (2H, s, Ar−H), 3.98−3.93 (6H, m, CH_2O), 2.99 (1H, s, C≡CH), 1.81−1.76 (6H, m, CH_2), 1.49−1.30 (18H, m, CH_2), 0.92−0.88 (9H, m, CH_3). ^{13}C NMR ($CDCl_3$, 75 MHz, ppm): δ 152.9, 139.5, 116.4, 110.6, 84.0, 75.7, 73.5, 69.1, 31.7, 31.5, 30.2, 29.2, 25.7, 22.64, 22.58, 14.03, 13.98. MS (EI), m/z: 402 (M^+, 100%). HRMS (EI): calcd for $C_{26}H_{42}O_3$: 402.3134. Found: 402.3136.

5: To A mixture of compound **4** (2.00 g, 4.98 mmol), 1,4-dibromo-2,5-diiodobenzene (1.16 g, 2.37 mmol) in a mixture of THF (80 mL) and Et_3N (20 mL) was added $Pd(PPh_3)_2Cl_2$ (200 mg) and CuI (20 mg). The mixture was stirred at 35 °C overnight. The reaction was quenched with NH_4Cl(aq). The organic layer was extracted with CH_2Cl_2. The combined extracts were washed with brine and dried over Na_2SO_4. After removal of the solvent under reduced pressure, the residue was purified by column chromatography (silica gel, CH_2Cl_2/petroleum ether = 1:3 as eluent) to afford a white solid (2.27 g). The white solid was dissolved in THF (80 mL) and water (10 mL), and then to this solution were added phenylboronic acid (588 mg, 4.82 mmol), $Pd(PPh_3)_4$ (202 mg, 0.175 mmol), and sodium carbonate (1.54 g, 14.5 mmol). The mixture was refluxed overnight. After quenched with NH_4Cl(aq), the mixture was extracted with CH_2Cl_2. The combined extracts were washed with brine and dried over anhydrous Na_2SO_4. After removal of the solvents at reduced pressure, the residue was purified by column chromatography (silica gel, CH_2Cl_2:petroleum ether = 1:3 as eluent) to afford **5** (2.10 g) as a white solid. Yield: 86% for two steps. ^{1}H NMR ($CDCl_3$, 300 MHz, ppm): δ 7.75−7.69 (6H, m, Ar−H), 7.51−7.46 (4H, m, Ar−H), 7.42−7.39 (2H, m, Ar−H), 6.51 (4H, s, Ar−H), 3.96−3.89 (12H, m, CH_2O), 1.81−1.70 (12H, m, CH_2), 1.49−1.29 (36H, m, CH_2), 0.94−0.87 (18H, m, CH_3).

^{13}C NMR ($CDCl_3$, 75 MHz, ppm): δ 152.9, 142.4, 139.7, 139.2, 133.3, 129.4, 127.9, 127.6, 121.6, 117.5, 109.9, 94.4, 88.1, 73.5, 69.0, 31.7, 31.5, 30.2, 29.2, 25.7, 22.7, 22.6, 14.1, 14.0. MALDI-TOF MS, *m*/*z*: 1031 (M^+). Anal. Calcd for $C_{70}H_{94}O_6$: C, 81.51; H, 9.19. Found: C, 81.26; H, 9.41.

6: To a solution of **5** (1.00 g, 0.97 mmol) in 80 mL of CH_2Cl_2 was added a solution of ICl (347 mg, 2.14 mmol) in CH_2Cl_2 dropwise at −78 °C. After 10 min, $Na_2S_2O_3$(aq) was added to remove the excess ICl, and then the mixture was extracted with $CHCl_3$. The extracts were washed with brine and dried over anhydrous Na_2SO_4. After removal of the solvent under reduced pressure, the residue was purified by column chromatography (silica gel, $CHCl_3$/petroleum ether = 1:3 as eluent) to afford **6** (1.23 g) as a white solid. Yield: 99%. ^{1}H NMR (300 MHz, $CDCl_3$, ppm): δ 9.81 (s, 1H, Ar−H), 9.00−8.97 (d, 2H, J = 8.4 Hz, Ar−H), 7.79−7.74 (m, 2H, Ar−H), 7.61−7.52 (m, 4H, Ar−H), 6.55 (s, 4H, Ar−H), 4.16−4.12 (t, 4H, J = 6.3 Hz, CH_2O), 4.04−3.97 (m, 4H, CH_2O), 1.89−1.78 (m, 12H, CH_2), 1.58−1.25 (m, 36H, CH_2), 0.97−0.87 (m, 18H, CH_3). ^{13}C NMR ($CDCl_3$, 75 MHz, ppm): δ 153.1, 146.5, 140.1, 137.9, 132.5, 131.3, 130.1, 129.7, 129.1, 127.6, 123.0, 108.5, 106.4, 73.6, 69.2, 31.8, 31.6, 30.4, 29.7, 29.3, 25.8, 25.7, 22.7, 22.6, 14.1, 14.0. MALDI-TOF MS, *m*/*z*: 1157 ([M − I]$^+$). Anal. Calcd for $C_{70}H_{92}I_2O_6$: C, 65.52; H, 7.23. Found: C, 65.17; H, 7.35.

7: To A mixture of 2,7-dibromo-9,9-dihexylfluorene (3.00 g, 6.12 mmol) and 4-formylphenylboronic acid (2.02 g, 13.5 mmol) in THF (80 mL) was added $Pd(PPh_3)_2Cl_2$ (180 mg). The mixture was stirred at 85 °C overnight. After the mixture was quenched with aqueous NH_4Cl, the aqueous layer was extracted with EtOAc. The combined extracts were washed with brine and dried over Na_2SO_4. After removal of the solvent at reduced pressure, the residue was purified by column chromatography (silica gel, ethyl acetate/petroleum ether = 1:15 as eluent) to afford **7** (3.25 g) as a white solid. Yield: 98%. ^{1}H NMR ($CDCl_3$, 300 MHz, ppm): δ 10.08 (1H, s, Ar−H), 8.01−7.98 (4H, m, Ar−H), 7.85−7.82 (6H, m, Ar−H), 7.68−7.63 (4H, m, Ar−H), 2.10−2.04 (4H, m, Ar−CH_2), 1.12−1.07 (12H, m, CH_2), 0.77−0.73 (10H, m, CH_3). ^{13}C NMR ($CDCl_3$, 75 MHz, ppm): δ 191.8, 151.8, 141.8, 140.3, 139.2, 132.7, 128.8, 127.0, 126.1, 121.4, 120.2, 87.6, 55.3, 40.4, 31.4, 29.7, 23.8, 22.5, 14.0. MS (EI), *m*/*z*: 542 (M^+, 100%). HRMS (EI): calcd for $C_{39}H_{42}O_2$: 542.3185. Found: 542.3187.

8: A mixture of CBr_4 (3.68 g, 11.1 mmol) and PPh_3 (5.95 g, 22.7 mmol) in 50 mL of CH_2Cl_2 was stirred at 0 °C for 1 h under a N_2 atmosphere, and then a solution of compound **7** (3.00 g, 5.54 mmol) in 30 mL of CH_2Cl_2 was added dropwise. The mixture was stirred at room temperature overnight. The mixture was filtrated, and the solution was collected. After the removal of solvent at reduced pressure, the residue was purified by a chromatography on silica gel using ethyl acetate/petroleum ether (1:40) to give **8** as a white solid (4.56 g, 5.37 mmol). Yield: 97%. ^{1}H NMR (300 MHz, $CDCl_3$, ppm): 7.79−7.54 (m, 16H, Ar−H), 2.07−2.01 (m, 12H, CH_2), 1.14−1.06 (m, 12H, CH_2), 0.77−0.72 (m, 10H, CH_3). ^{13}C NMR ($CDCl_3$, 75 MHz, ppm): δ 151.8, 141.6, 140.3, 139.2, 136.4, 134.0, 128.8, 127.0, 126.0, 121.2, 120.2, 89.4, 55.3, 40.4, 31.4, 29.7, 23.8, 22.5, 14.0. MS (EI), *m*/*z*: 850 (M^+, 100%). HRMS (EI): calcd for $C_{41}H_{42}Br_2$: 850.0020. Found: 850.0022.

9: To a solution of **8** (4.00 g, 4.71 mmol) in 80 mL of anhydrous THF was added *n*-BuLi (5.65 mL, 14.1 mmol) at −78 °C, and the solution was stirred at −78 °C for another 3 h. The mixture was quenched with NH_4Cl(aq). The aqueous layer was extracted with CH_3COOEt. The combined organic extracts were washed with brine and dried over Na_2SO_4. After removal of the solvents under reduced pressure, the residue was purified by a chromatography on silica gel using CH_2Cl_2/petroleum ether = 1:4 to give **9** as a white solid (2.44 g). Yield: 97%. ^{1}H NMR ($CDCl_3$, 300 MHz, ppm): δ 7.79−7.55 (14H, m, Ar−H), 3.15 (1H, s, C≡CH), 2.06−2.00 (4H, m, CH_2), 1.11−1.00 (12H, m, CH_2), 0.77−0.72 (10H, m, CH_3). ^{13}C NMR ($CDCl_3$, 75 MHz, ppm): δ 151.8, 141.9, 140.3, 139.2, 132.5, 127.0, 126.1, 121.3, 120.8, 120.2, 83.6, 55.3, 40.4, 31.4, 29.6, 23.8, 22.5, 14.0. MS (EI), *m*/*z*: 534 (M^+, 100%). HRMS (EI): calcd for $C_{41}H_{42}$: 534.3287, Found: 534.3290.

Polymer **P**: To a mixture of **6** (321 mg, 0.25 mmol), **9** (139 mg, 0.26 mmol), $Pd(PPh_3)_4$ (29 mg), and CuI (10 mg) were placed in a 50 mL flask. The flask was evacuated and backfilled with nitrogen three times, followed by the addition of anhydrous toluene (20 mL) and *i*-Pr_2NH (7 mL). The mixture was stirred at 75 °C for 2 days. The mixture was subjected to a CH_2Cl_2/H_2O work-up. The combined organic layer was washed with saturated aqueous NH_4Cl and dried over Na_2SO_4. After the solvent was removed under vacuum, the combined extracts were washed with brine and dried over Na_2SO_4. After removal of the solvent at reduced pressure, the residue dissolved in chloroform was reprecipitated in methanol. The precipitate was filtered and washed with MeOH to give a yellow fibrous solid (236 mg). Removal of the impurities was achieved by subjecting the solid to sequential extractions in a Soxhlet extractor with acetone. The resulting solid was resolved in chloroform and reprecipitated in methanol again to afford polymer **P** (197 mg, 50%) as a yellow solid. ^{1}H NMR ($CDCl_3$, 300 MHz, ppm): δ 10.06 (2H, br, Ar−H), 9.06 (2H, br, Ar−H), 7.83−7.31 (20H, br, Ar−H), 6.86−6.83 (6H, br, Ar−H), 4.20−4.04 (12H, br, CH_2O), 2.09−1.12 (68H, br, CH_2), 0.95−0.78 (24H, br, CH_3). ^{13}C NMR ($CDCl_3$, 75 MHz, ppm): δ 152.8, 151.8, 143.8, 139.2, 137.5, 134.5, 132.8, 131.9, 130.3, 129.4, 128.3, 127.0, 125.9, 122.8, 121.2, 120.1, 109.1, 73.5, 69.1, 55.2, 40.4, 31.7, 31.4, 30.3, 29.6, 29.2, 25.8, 25.7, 23.7, 22.6, 22.5, 14.0, 13.9.

Acknowledgment. We thank Prof. Dechun Zou and Xing Fan of Peking University for help of setting up the electrospinning apparatus. We also acknowledge Dr. Lei Ye of Lund University and Prof. Dahui Zhao of Peking University for helpful discussions. This work was supported by the National Natural Science Foundation of China (20675003, 90713013, J0630421) and Instrumental Analysis Fund of Peking University.

References and Notes

(1) (a) Swager, T. M. *Acc. Chem. Res.* **1998**, *31*, 201–207. (b) McQuade, D. T.; Pullen, A. E.; Swager, T. M. *Chem. Rev.* **2000**, *100*, 2537–2574. (c) Thomas, S. W.; Joly, G. D.; Swager, T. M. *Chem. Rev.* **2007**, *107*, 1339–1386. (d) Larsen, G.; Velarde-Ortiz, R.; Minchow, K.; Barrero, A.; Loscertales, I. G. *J. Am. Chem. Soc.* **2003**, *125*, 1154–1155. (e) Zhao, Y.; Cao, X.; Jiang, L. *J. Am. Chem. Soc.* **2007**, *129*, 764–765. (f) Singh, A.; Steely, L.; Allcock, H. R. *Langmuir* **2005**, *21*, 11604–11607.

(2) (a) Yang, J.; Swager, T. M. *J. Am. Chem. Soc.* **1998**, *120*, 11864–11873. (b) Zhou, Q.; Swager, T. M. *J. Am. Chem. Soc.* **1995**, *117*, 7017–7018. (c) Yang, J.; Swager, T. M. *J. Am. Chem. Soc.* **1998**, *120*, 5321–5322. (c) Sanchez, J. C.; Urbas, S. A.; Toal, S. J.; DiPasquale, A. G.; Rheingold, A. L.; Trogler, W. C. *Macromolecules* **2008**, *41*, 1237–1245. (d) Sanchez, J. C.; DiPasquale, A. C.; Rheingold, A. L.; Trogler, W. C. *Chem. Mater.* **2007**, *19*, 6459–6470.

(3) (a) Li, M. J.; Zhang, J. H.; Zhang, H.; Liu, Y. F.; Wang, C. L.; Xu, X.; Tang, Y.; Yang, B. *Adv. Funct. Mater.* **2007**, *17*, 3650–3656. (b) Moroni, L.; Schotel, R.; Hamann, D.; de Wijn, J. R.; Van Blitterswijk, C. A. *Adv. Funct. Mater.* **2008**, *18*, 53–60. (c) Li, Z. Y.; Zhang, H. N.; Zhang, W.; Wang, W.; Huang, H. M.; Wang, C.; Macdiarmid, A. G.; Wei, Y. *J. Am. Chem. Soc.* **2008**, *130*, 5036–5037.

(4) Megelski, S.; Stephens, J. S.; Chase, D. B.; Rabolt, J. F. *Macromolecules* **2002**, *35*, 8456–8466.

(5) (a) Zhao, D. H.; Swager, T. M. *Macromolecules* **2005**, *38*, 9377–9384. (b) Gibson, P.; Gibson, H. S.; Rivin, D. *Colloids Surf., A* **2001**, *187*, 469–481. (c) He, F.; Tang, Y.; Wang, S.; Li, Y.; Zhu, D. *J. Am. Chem. Soc.* **2005**, *127*, 12343–12346. (d) Xu, Q.; Wang, S.; Mikhailovsky, A.; Bazan, G. C.; Moses, D.; Heeger, A. J. *Proc. Natl. Acad. Sci. U.S.A.* **2005**, *102*, 530–535. (e) Wang, S.; Liu, B.; Gaylord, B. S.; Bazan, G. C. *Adv. Funct. Mater.* **2003**, *13*, 463–467. (f) Liu, B.; Gaylord, B. S.; Wang, S.; Bazan, G. C. *J. Am. Chem. Soc.* **2003**, *125*, 6705–6714.

(6) (a) Yang, J.; Swager, T. M. *J. Am. Chem. Soc.* **1998**, *120*, 11864–11873. (b) Zhou, Q.; Swager, T. M. *J. Am. Chem. Soc.* **1995**, *117*,

7017–7018. (c) Yang, J.; Swager, T. M. *J. Am. Chem. Soc*. **1998**, *120*, 5321–5322.
(7) (a) Sanchez, J. C.; Urbas, S. A.; Toal, S. J.; DiPasquale, A. G.; Rheingold, A. L.; Trogler, W. C. *Macromolecules* **2008**, *41*, 1237–1245. (b) Sanchez, J. C.; DiPasquale, A. C.; Rheingold, A. L.; Trogler, W. C. *Chem. Mater*. **2007**, *19*, 6459–6470.
(8) Saxena, A.; Fujiki, M.; Rai, R.; Kwak, G. *Chem. Mater*. **2005**, *17*, 2181–2185.
(9) (a) Greiner, A.; Wendorff, J. H. *Angew. Chem., Int. Ed*. **2007**, *46*, 5670–5703. (b) Li, D.; Xia, Y. N. *Adv. Mater*. **2004**, *16*, 1151–1170. (c) Li, D.; Babel, A.; Jenekhe, S. A.; Xia, Y. N. *Adv. Mater*. **2004**, *16*, 2062–2066.
(10) (a) Patel, A. C.; Li, S. X.; Yuan, J. M.; Wei, Y. *Nano Lett*. **2006**, *6*, 1042–1046. (b) Matthews, J. A.; Wnek, G. E.; Simpson, D. G.; Bowlin, G. L. *Biomacromolecules* **2002**, *3*, 232–238. (c) Caruso, R. A.; Schattka, J. H.; Greiner, A. *Adv, Mater*. **2000**, *13*, 1577–1579. (d) Jiang, L.; Zhao, Y.; Zhai, J. *Angew. Chem., Int. Ed*. **2004**, *43*, 4338–4341. (e) Zhu, Y.; Zhang, J. C.; Zheng, Y. M.; Huang, Z. B.; Feng, L.; Jiang, L. *Adv. Funct. Mater*. **2006**, *16*, 568–574.
(11) (a) Wang, X. Y.; Drew, C.; Lee, S. H.; Senecal, K. J.; Kumar, J.; Samuelson, L. A. *Nano Lett*. **2002**, *2*, 1273–1275. (b) Wang, X. Y.; Kim, Y. G.; Drew, C.; Ku, B. C.; Kumar, J.; Samuelson, L. A. *Nano Lett*. **2004**, *4*, 331–334. (c) Tao, S. Y.; Li, G. T.; Yin, J. X. *J. Mater. Chem*. **2007**, *17*, 2730–2736.
(12) Li, M. J.; Zhang, J. H.; Zhang, H.; Liu, Y. F.; Wang, C. L.; Xu, X.; Tang, Y.; Yang, B. *Adv. Funct. Mater*. **2007**, *17*, 3650–3656.
(13) Yao, T.; Campo, M. A.; Larock, R. C. *J. Org. Chem*. **2005**, *70*, 1432–1437.
(14) Gibson, P.; Gibson, H. S.; Rivin, D. *Colloids Surf., A* **2001**, *187*, 469–481.